Photocatalytic inactivation of Enterobacter cloacae and Escherichia coli using titanium dioxide supported on two substrates

Aguas, Y., Hincapie, M., Sanchez, C., Botero, L., & Fern��ndez-Ib����ez, P. (2018). Photocatalytic inactivation of Enterobacter cloacae and Escherichia coli using titanium dioxide supported on two substrates. *Processes*, *6*(9), [6]. https://doi.org/10.3390/pr6090137

Link to publication record in Ulster University Research Portal

Published in:
Processes

Publication Status:
Published (in print/issue): 23/08/2018

DOI:
10.3390/pr6090137

Document Version
Author Accepted version

General rights
Copyright for the publications made accessible via Ulster University's Research Portal is retained by the author(s) and / or other copyright owners and it is a condition of accessing these publications that users recognise and abide by the legal requirements associated with these rights.

Take down policy
The Research Portal is Ulster University's institutional repository that provides access to Ulster's research outputs. Every effort has been made to ensure that content in the Research Portal does not infringe any person's rights, or applicable UK laws. If you discover content in the Research Portal that you believe breaches copyright or violates any law, please contact pure-support@ulster.ac.uk.

Download date: 05/05/2023

processes

MDPI

Article

Photocatalytic Inactivation of *Enterobacter cloacae* and *Escherichia coli* Using Titanium Dioxide Supported on Two Substrates

Yelitza Aguas [1,2,*], Margarita Hincapié [2], Camilo Sánchez [3], Liliana Botero [2] and Pilar Fernández-Ibañez [4]

1 School of Engineering, Universidad de Sucre, Sincelejo 700001, Colombia
2 School of Engineering, Universidad de Medellín, Medellín 050026, Colombia; mhincapie@udem.edu.co (M.H.); lbotero@udem.edu.co (L.B.)
3 School of Engineering, Universidad de Antioquia, Medellín 050010, Colombia; ksatoiq@gmail.com
4 Nanotechnology and Integrated BioEngineering Centre, School of Engineering, University of Ulster, Newtownabbey BT37 0QB, Northern Ireland, UK; p.fernandez@ulster.ac.uk
* Correspondence: yelitza.aguas@unisucre.edu.co; Tel.: +11-575-2826507

Received: 1 July 2018; Accepted: 16 August 2018; Published: 23 August 2018

Abstract: The antibacterial photocatalytic activity of TiO_2 supported over two types of substrates, borosilicate glass tubes (TiO_2/SiO_2-borosilicate glass tubes (BGT)) and low-density polyethylene pellets (TiO_2-LDPE pellets), which were placed in a compound parabolic collectors (CPC) reactor, was evaluated against *Enterobacter cloacae* and *Escherichia coli* under sunlight. Three solar photocatalytic systems were assessed, suspended TiO_2, TiO_2/SiO_2-BGT and TiO_2-LDPE pellets, at three initial bacterial concentrations, 1×10^5; 1×10^3; 1×10^1 CFU/mL of *E. coli* and total bacteria (*E. cloacae* and *E. coli*). The solar photo-inactivation of *E. coli* was achieved after two hours with 7.2 kJ/L of UV-A, while total bacteria required four hours and 16.5 kJ/L of UV-A. Inactivation order of *E. coli* was determined, as follows, suspended TiO_2/sunlight (50 mg/L) > TiO_2-LDPE pellets/sunlight (52 mg/L) > TiO_2/SiO_2-BGT/sunlight (59 mg/L), the best *E. coli*. inactivation rate was obtained with TiO_2-LDPE pellets/sunlight, within 4.5 kJ/L and 90 min. The highest total bacteria inactivation rate was found for TiO_2/sunlight (50 mg/L) and TiO_2-LDPE pellets/sunlight (52 mg/L), within 11.2 kJ/L and 180 min. TiO_2 deposited over LDPE pellets was the most effective material, which can be successfully used for water disinfection applications. Bacterial regrowth was assessed 24 h after all photocatalytic treatments, none of those microorganisms showed any recovery above the detection limit (2 CFU/mL).

Keywords: heterogeneous photocatalysis; supported TiO_2; *Enterobacter cloacae*; *Escherichia coli*; solar disinfection

1. Introduction

Recent research is focused on the use of advanced oxidation processes (AOPs) to disinfect water while using solar energy [1–3]. AOPs are processes that involve the generation of strong oxidizing and short life-time species, fundamentally hydroxyl radical •OH, which have a high redox potential (2.80 eV). Nevertheless, bacterial inactivation mechanism by AOPs involves several reactive oxygen species (ROS), including not only hydroxyl radicals, but also singlet oxygen or hydrogen peroxide. The systematic mechanisms and triggers that conduct bacterial death by the use of AOPs still remain unclear, and all points out that it depends on the type of photo-catalyst that is used [4,5]. Even in the absence of any catalyst, the action of solar UV photons induces the generation of a series of ROS at intracellular level producing both lethal and sub-lethal damages over bacteria [6]. Specifically, in the

case of heterogeneous photocatalysis, it is widely accepted that the first place for oxidative damage occurs in the external cell membrane of microorganisms [7].

TiO_2 is the most used material in these processes because of its high photocatalytic activity, stability, and safety [8]. The efficiency of heterogeneous photocatalysis is based on the photo-activation of TiO_2 (λ < 385 nm). This photoactivation induces the generation of electron-hole pairs at the semiconductor, an electron is promoted from the valence band to the conduction band (e^-), generating a hole (h^+) on the valence band. Then, redox reactions in an aqueous medium produce reactive oxygen species as hydroxyl radicals ($^\bullet OH$), superoxide radicals ($O_2^{\bullet -}$), and hydrogen peroxide (H_2O_2), via a series of surface reactions, producing oxidative radicals that stress microorganisms to different target sites (i.e., surface and cell wall), and thereafter producing lethal damages to them [1,2,9].

TiO_2 is usually used in suspension, nevertheless this kind of application has some disadvantages, such as crowding, aggregation, and the later separation of the photocatalyst after the reactions from the liquid phase to recover and reuse it in further photocatalytic applications. For this reason, a number of contributions on the immobilization of the TiO_2 on a substrate have been developed [10,11]. TiO_2 can be supported on various inert substrates such as glass, polymers, quartz, and metals, depending on the technique that is used for the impregnation process and photo reactor set up. Coated materials generally have a lower active surface area with lower oxidation activity in comparison with suspended TiO_2 [11,12]. Characteristics of the substrates, including porosity, mechanical, chemical and thermal resistance, and photo corrosion should be considered, as they are key to facilitate the adherence and effectiveness of the catalyst [13]. Among the catalyst immobilization methods available, sol-gel [10,11,13], alkaline hydrothermal synthesis [14], the binding agent [15], dip coating [16,17], deposition in a liquid phase [18], chemical vapor deposition [19], dispersion for thermal encapsulation [20], and supported on polymers have been used [21].

Research on water disinfection have investigated supported TiO_2 on different substrates, including glass tubes, where TiO_2 films over glass cylinders were prepared using the sol-gel method for inactivating total and fecal coliforms [7] and *Alteromonas* sp. and *Corynebacterium stationis* [22]. TiO_2 Films of photocatalyst immobilized by dip coating over the inner of walls of glass reactors [15], as well as in glass raschig rings were used to successfully inactivate *E. coli* [11,13,16]. TiO_2 supported on glass nanotubes, nanoplates, nanorods, and nanospheres, as elaborated by the alkaline hydrothermal method, were applied for the *Fusarium solani* treatment [11]. TiO_2 was immobilized on stainless steel helical support by electrostatic spraying method to *E. coli* inactivation [23].

Polymers have been also used as substrates for the immobilization of TiO_2. Low density polyethylene (LDPE)-TiO_2 films were produced by an extrusion method for the degradation of methylene blue and inactivation of *E. coli* [24] and by sputtered for 8 min with surface RF-plasma and UV-C pretreatments applying in *E. coli* inactivation [25]. TiO_2 coating by heat treatment on high-density polyethylene (HDPE) cutting board through [26] was evaluated for *E. coli* inactivation [27]. *Staphylococcus aureus* and *Escherichia coli* were treated using polypropylene/titanium dioxide (PP/TiO_2) nanocomposites that were prepared by the sol-gel method [28].

These supported catalysts are usually configured in static systems, including those that are supported on raschig rings. TiO_2 has also been supported on flow systems such as polymer pellets that allow the photocatalyst to have mobility within the reactor but immobilized over substrates, and consequently allowing for an easy reuse after water treatment as well as easy recovery of the catalyst for cleaning or disposal [20]. The efficiency of these TiO_2 supported systems have been evaluated for the oxidation of organic compounds in water, nevertheless their photocatalytic activity for bacteria inactivation is still unknown or scarcely studied.

The aim of this work was to evaluate the photocatalytic efficiency of TiO_2 (P25, Evonik) immobilized on borosilicate glass tubes (BGT) and low-density polyethylene pellets (LDPE pellets), as efficient, mobile, and versatile materials, when compared with suspended TiO_2 (P25, Evonik), in a solar CPC reactor under natural sunlight, in the inactivation of *E. cloacae* and *E. coli*, as target bacteria.

2. Materials and Methods

2.1. Chemicals

Commercial TiO_2 (P25, Evonik, Germany) (anatase/rutile = 80/20) with a mean particle size of 20 to 30 nm was used for photocatalytic experiments with 3.8 g/cm^3 of density and 50 m^2/g of specific surface area approximately. Glycerin (USP) was used for thermal encapsulation and tetraethyl orthosilicate ($Si(OC_2H_5)_4$, 99%, Merck, Germany), 2-propanol ($(CH_3)_2CHOH$, 99.8%, JT Backer, USA), hydrochloric acid (HCl, 36%, Merck), and sulfuric acid (H_2SO_4, 96%, Mallinckrodt, USA) for the sol-gel method. Borosilicate glass tubes (BGT) (L = 28 cm y d = 1.0 cm, TQ Laboratorios, Colombia) and low-density polyethylene (LDPE) pellets (2 mm, DNDA8320, Químicos y Plásticos Industriales S.A., Colombia) were used as supports.

2.2. Bacterial Strains, Preparation and Quantification

Two bacterial strains were selected for photocatalytic tests, *Enterobacter cloacae* ATCC 13047 and *Escherichia coli* ATCC 25922, which were spiked in distilled water. *Enterobacter cloacae* and *Escherichia coli* strains were cultivated by an extension method in nutrient agar (Merck) and incubated at 37 ± 0.5 °C for 18 h to reach stationary growth phase. After 18 hours of incubation, the concentration of bacteria of 10^9 CFU/mL.

The water samples were filtered through nitrocellulose 47 mm filters with 0.45 m pore size (Sartorius AG, Germany). The filter was placed on Agar Cromocoulth (Merck, Germany) and incubated at 37.0 ± 0.5 °C for 24 h. The samples with less content of bacteria were undiluted plated in petri dishes at volumes of 500 L for a detection limit of 2 CFU/mL.

2.3. TiO_2/SiO_2-BGT

BGT was previously treated with H_2SO_4 3 M to remove all the impurities that could migrate to the film and act as a recombination center, reducing the photocatalytic activity of TiO_2 and hindering the good adherence of the film [18]. A gel to obtain a silica matrix was prepared while using tetraethyl orthosilicate, water and 2-propanol, with molar ratios of water:tetraethyl orthosilicate = 3 and 2-propanol:water = 3.5. Additionally, 0.3 mL of HCl 3 M was added as the reaction initiator, according to the method to deposit TiO_2/SiO_2 layers on BGT by Granda et al. [29]. The gel was mixed for 90 min and then it was aged for 24, 36, 48, and 60 h before starting film deposition. TiO_2 was dispersed in the gel at 10,000 rpm. TiO_2/SiO_2 films were supported on the tubes through a dip coating procedure with a controlled speed at 15 cm/min. Afterwards, the supported tubes were thermally processed (100 °C) for 4 h. Then, they were washed in distilled water to remove all of the non-supported particles [29].

2.4. TiO_2-LDPE Pellets

TiO_2 was dispersed on glycerin at a mass concentration of 12.5% *w/w* (sol). The sol was heated up to 106 °C for the softening of the LDPE pellets and the system was shaken for 30 min, followed by a cooling step to room temperature, according to the controlled-temperature embedding method published elsewhere [20]. The layers of TiO_2 were deposited on the LDPE pellets, following the same methodology and adding 0.6 g of the photocatalyst in the TiO_2/glycerin system after each cooling step, with the purpose of obtaining coated materials with 1, 2, 3, 4, and 5 layers. The coated LDPE pellets were washed in cold water and dried at room temperature for 24 h, after each layer deposition process.

2.5. Characterization of Films

The morphology of coated films on BGT and LDPE pellets were characterized by scanning electron microscopy (SEM) while using a JEOL JSM-6490LV microscope, Japan. TiO_2-LDPE pellets were analyzed by Fourier Transform infrared spectroscopy equipped with attenuated total reflectance

unit (FTIR-ATR) using an IR Prestige-21, Shimadzu spectrometer, Japan, obtaining spectra ranging between 4000 and 500 cm^{-1}. The TiO2 amount coated per gram of pellet was determined through thermal gravimetric analysis (TGA) using 20 g of pellets that were submitted to a temperature program, between 25 °C to 1000 °C with a heating rate of 10 °C/min, where the residual weight corresponded to the amount of coated TiO_2 over the pellet. The surface atomic Ti percentage on the BGT was determined by energy dispersive X-ray spectroscopy (EDS), Japan, analyses performance in the JEOL microscope described above, while coated TiO_2 amount was determined by atomic absorption analysis (AA) in a thermo Scientific ICE Serie 3000 spectrophotometer, acetylene-nitrous oxide flame, after a digested with hydrofluoric acid.

The mechanical resistance of the films in the systems TiO_2/SiO_2-BGT and TiO_2-LDPE pellets was evaluated through erosion tests while using a Ney Ultrasonik 57H. Both of the systems were immersed in a solution of isopropanol-water 1:1 during 30 min under sonication and then dried at 25 °C for 24 h. By weighing before and after sonication process, the weight loss of the film was determined.

2.6. Solar CPC Photo-Reactor

For solar photo-catalytic experiments, a solar compound parabolic collector (CPC) reactor was used. The reflecting surface of the reactor is composed by a CPC built in 1 mm caliber, 25 cm wide, and 12 cm high aluminum. An acrylic crystal tube transparent was use as photoreactor. The material transmits 60−90% in the range 300−400 nm, with a cut-off wavelength of 290 nm. The tube, with 6 cm exterior diameter, 6 mm of thickness, and 60 cm of length, was placed in the focal line of the CPC mirror. The immobilized photocatalytic materials were placed inside the photo reactor according to their geometrical characteristics, i.e., 42 TiO_2/SiO_2-BGT (59 mg/L TiO_2), and 650 g of TiO_2-LEPD pellets (52 mg/L TiO_2) were packed. The CPC reactor was located on a supporting platform inclined 6° with regard to the horizontal, in Medellin, Colombia, and connected to a reservoir tank. A submersible pump at a flow rate of 11.7 L/min was used to recirculate the water (Figure 1). The reactor volume was 3 L, the illuminated volume 0.9 L, and the solar collector irradiated area was 0.067 m^2.

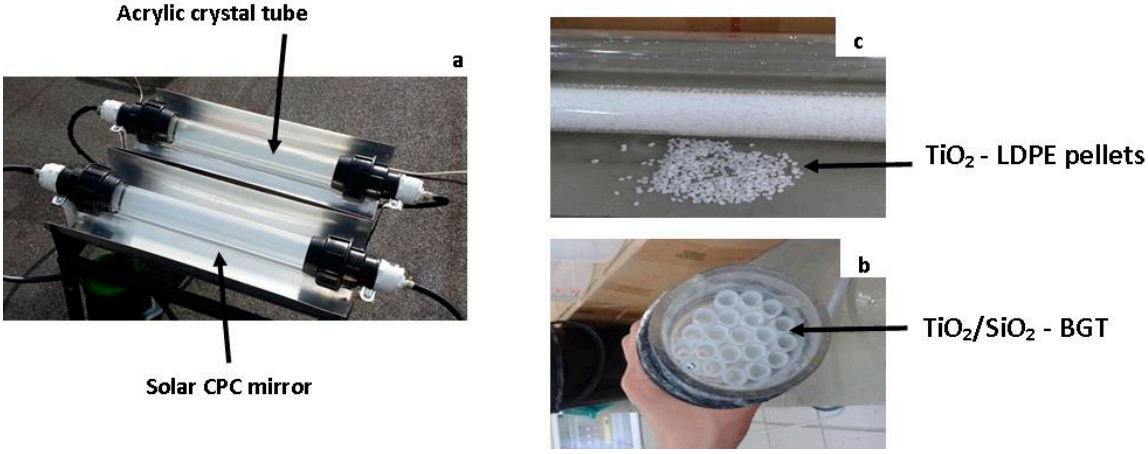

Figure 1. Photoreactor: (**a**) solar compound parabolic collector (CPC) reactor; (**b**) TiO_2/SiO_2-borosilicate glass tubes (BGT); and (**c**) TiO_2-low density polyethylene (LDPE) pellets.

2.7. Solar Photocatalytic Disinfection Experiments

For solar photocatalytic tests, three types of photocatalytic system, suspended TiO_2, TiO_2/SiO_2-BGT and TiO_2-LDPE pellets. Three initial bacterial concentrations, 1×10^5; 1×10^3; 1×10^1 CFU/mL of *E. coli* and *E. cloacae*, were evaluated. Initially, the microorganism suspensions were placed in the reservoir tank and circulated for 15 min in the dark for homogenization. Prior to solar exposure, the first sample was taken and the photo reactor was uncovered to start the solar photocatalytic treatment. Samples of 10 mL were taken every 15 min for a period of 4 h.

Temperature, pH, dissolved oxygen in water, and solar UV-A irradiance were monitored in situ during the experiments.

The effect of the solar radiation, and the mechanical stress due to the movement of the LDPE pellets in the viability of bacteria, at an initial concentration of 10^5 CFU/mL of *E. coli* and total bacteria, were evaluated. The water pH varied from 6.1 and 7.2 during experiments, the temperature was below 35 °C and the dissolved oxygen varied between 7.1 and 8.2. These operating conditions have been demonstrated to have no significant detrimental effect over bacterial viability [30].

The UV-A solar radiation was measured using an UV-A Solar Light Company, Inc. PMA2100 Version 1.19 radiometer, USA, placed by the photo reactor at an inclination of 6°, the same than reactor inclination. Solar radiation was evaluated in terms of solar UV-A irradiance that is defined as the surface rate at which the incoming solar radiant energy reaches the surface ($W \cdot m^{-2}$). The solar UV-A dose received on the illuminated reactor surface (A_r, m^2), under a certain solar UV intensity (UV, $W \cdot m^{-2}$), and the accumulated UV-A energy per unit of treated water volume (Q_{UV}, $J \cdot L^{-1}$), which is frequently used for applications in solar reactors Equation (1) [8].

$$Q_{uv} = \Sigma_n UV_{n-1} \cdot \frac{A_r}{V_t} \cdot \Delta_{tn} \quad (1)$$

where t_n is the experimental time for n-sample (seconds), $\overline{UV}_{n-1}$ the average solar ultraviolet radiation that was measured during the period ($t_n - t_{n-1}$), A_r is the illuminated collector surface and V_t, the reactor total volume (L).

3. Results and Discussion

3.1. Characterization of TiO_2/SiO_2-BGT

Titanium percentages of TiO_2/SiO_2 film immobilized over BGT were determined by EDS analysis (Table 1). This analysis showed that the film obtained after 36 h of aging had the highest atomic percentage of Ti incorporated (1.49%) into the silica matrix and the best adhesion to the BGT, with only 0.01% of film losses. On the contrary, the lowest and highest aging times led to the lowest atomic percentages of Ti incorporated into the silica matrix. Therefore, 36 h of aging time was the optimum time for polymerization and it was selected for preparing the films of TiO_2/SiO_2 on BGT. Additionally, 4.24 mg of TiO_2 was immobilized on each BGT.

Table 1. Atomic percentages of Ti and Si, determined by energy dispersive X-ray spectroscopy (EDS) analysis, in TiO_2/SiO_2-borosilicate glass tubes (BGT), obtained after different time of the matrix silica aging.

Hours of Matrix Silica Aging	Atomic % Ti	Atomic % Si
24	1.08	41.49
36	1.49	32.39
48	1.13	39.77
60	1.10	40.40

Figure 2a,b shows SEM micrographs of an unsupported BGT and TiO2/SiO2-BGT (36 h of matrix silica aging), respectively. Although it can be seen small agglomerates of TiO_2/SiO_2, they are homogeneously dispersed, indicating an effective coating of TiO_2. These small agglomerates could be attributed to a low speed of immersion of the tube into the TiO_2/SiO_2 solution during the coating process, as has been reported by other authors [19,31]. On the other hand, EDS analysis (Figure 3) confirms that O, Si, and Ti are homogenously distributed over the surface. In addition, the higher concentration of Ti (Figure 3c) coincides with the found agglomerates in Figure 2b.

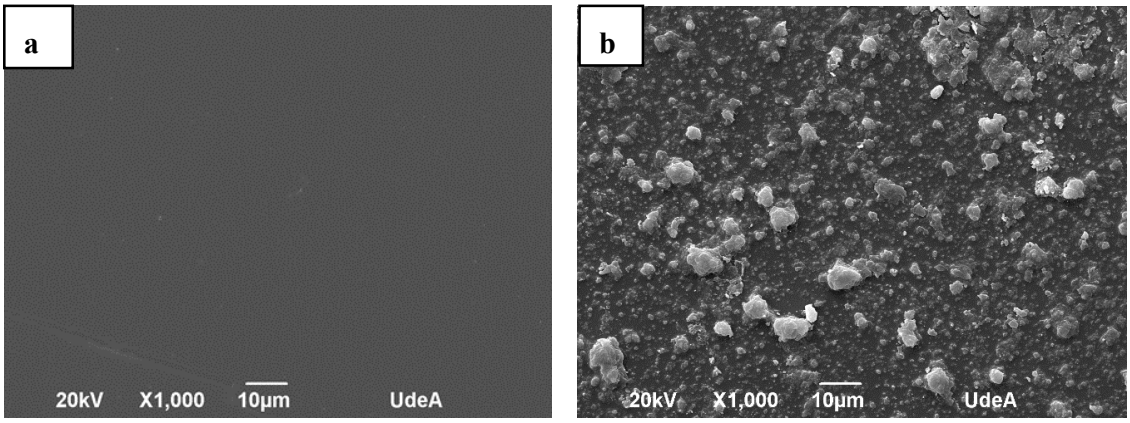

Figure 2. Scanning electron microscopy (SEM) images of (**a**) bare BGT and (**b**) TiO_2/SiO_2-BGT.

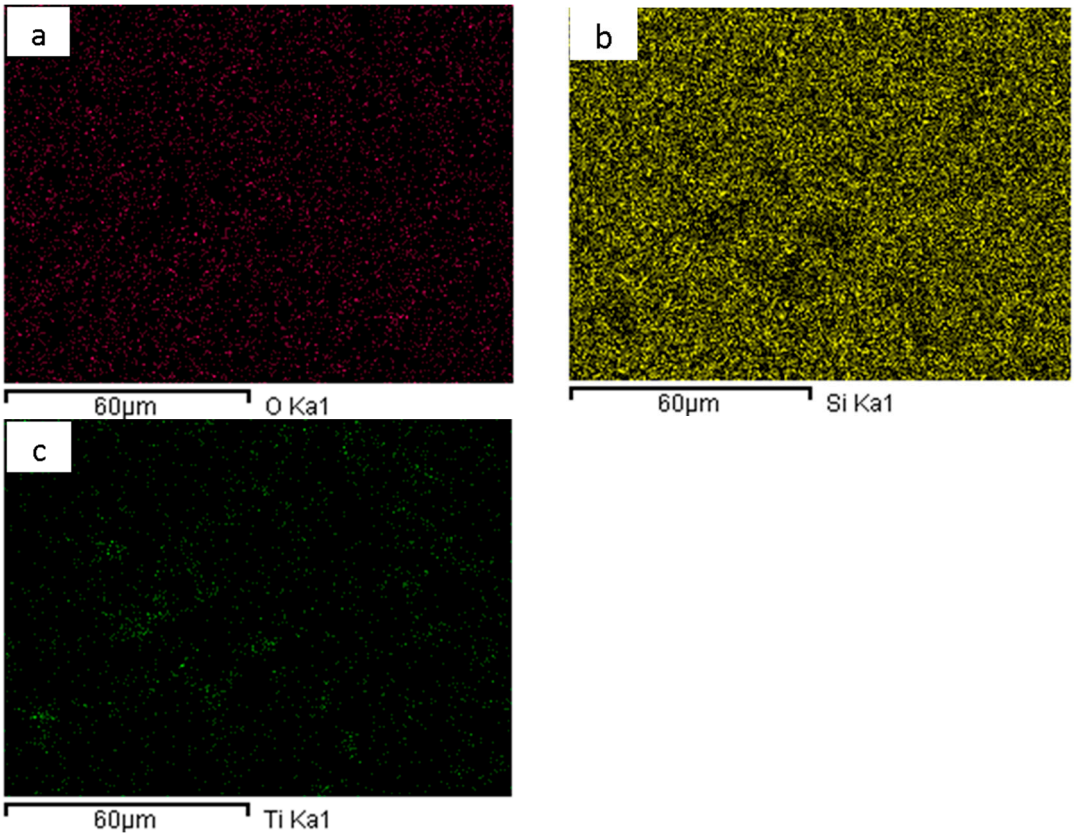

Figure 3. EDS images of TiO_2/SiO_2 films. Distributions of (**a**) O, (**b**) Si, and (**c**) Ti.

In the CPC reactor were located 42 TiO_2/SiO_2-BGT, organized in two packages in series with 21 tubes in parallel each one (Figure 1b), which was possible according to the capacity of the outer structure of the reactor and the high UV transmittance of the glass tube, as well as the thickness of the supported film that allowed for the path of the radiation to the catalyst located in the inner tube. A low flow rate of 11.7 L/min was selected to permit a good contact of the fluid and the immobilized catalyst, and therefore to allow for the contact or approximation of bacteria to the TiO_2/SiO_2-BGT surface

3.2. TiO_2-LDPE Pellets

Infrared spectra of LDPE pellets before and after impregnation are shown in Figure 4. In the IR spectrum of LDPE pellet before impregnation (blue line) shows 2914 cm^{-1}, 2851 cm^{-1}, 1462 cm^{-1}, and 720 cm^{-1} bands that may correspond to asymmetric stretching, symmetric stretching, and bending, respectively, of the CH_2 groups of LDPE. On the other hand, in the FTIR-ATR spectrum of LDPE pellet after impregnation (red line) the same bands and additional between 3700 and 3000 cm^{-1}, around 1600 cm^{-1} and 960−500 cm^{-1} are observed. These bands belong to the stretching vibration of OH on surface of TiO_2, bending vibration of superficial adsorbed water molecules, and bending vibration of O-Ti-O bond, respectively, indicating the successful coating of TiO_2 over the LDPE pellet [32,33]. The IR spectra peak around 1600 nm is related to the presence of TiO_2.

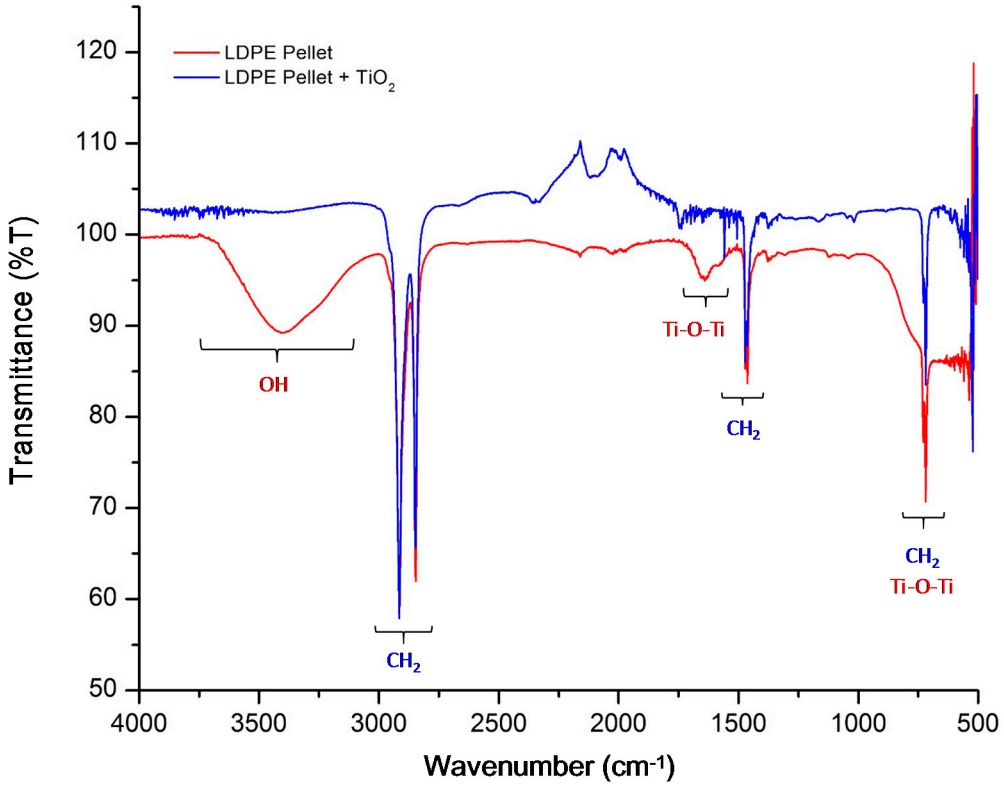

Figure 4. Fourier Transform infrared spectroscopy equipped with attenuated total reflectance unit (FTIR-ATR) spectra of bare pellet (blue line) and TiO_2-LDPE pellet (red line).

Thermal analysis revealed that the largest amount of the TiO_2 coated over the LDPE pellets was achieved in the first layer, and the amount of TiO_2 incorporated onto the pellets decreased when the number of layers increased, as shown in Table 2. This behavior could be attributed to changes in substrate properties when it is exposed to several heating cycles that are close to its melting temperature [34]. Also, it is possible that TiO_2 particles, which were gripped on the pellet during the first coating layer, could be released during the heating of subsequent coatings, giving, as a result, less amount of TiO_2 on the pellets with more layers. Thermal analysis also showed that the first layer contains 0.2374 mg of TiO_2 per gram of LDPE pellet, with only 0.1836% of coating losses. Other authors have reported similar results and indicated that immobilized TiO_2 particles were greatly imbedded and disperse well on the pellet when one layer was applied [17,23]. Therefore, TiO_2-LDPE pellets that were coated with one layer were selected to perform the photocatalytic experiments.

Table 2. Percentage of TiO_2 weight loss and amounts of TiO_2 incorporated on TiO_2-LPDE pellets with a different number of layers.

TiO_2-LDPE Pellets	% Weight Loss	mg TiO_2/g LDPE Pellets
1 layer	0.1836	0.2374
2 layers	0.1974	0.1495
3 layers	0.2253	0.1412
4 layers	0.2679	0.1080
5 layers	0.2884	0.0914

A large number of TiO_2-LDPE pellets were incorporated into the reactor due to its small size, which allows for easily adapting these systems to different configurations or reactor geometries. The density of the TiO_2-LDPE pellets allows for their dispersion in the treated water, making their mechanical behavior similar to the suspended photocatalyst. However, for very small flow, the supported pellets have the tendency to move to the upper wall of the reactor; for this reason, it is necessary to establish mechanical anchor systems to locate them in the bulk of the reactor.

SEM images of bare LDPE pellet and TiO_2-LDPE pellet (one-layer) are shown in the Figure 5. The TiO_2 particles are homogeneously dispersed over the surface of LDPE pellet with smaller agglomerates in comparison to TiO_2/SiO_2-BGT. Additionally, an EDS analysis displays a homogeneous distribution of titanium (Figure 6) on the surface pellet, confirming the homogeneous and successful coating of TiO_2.

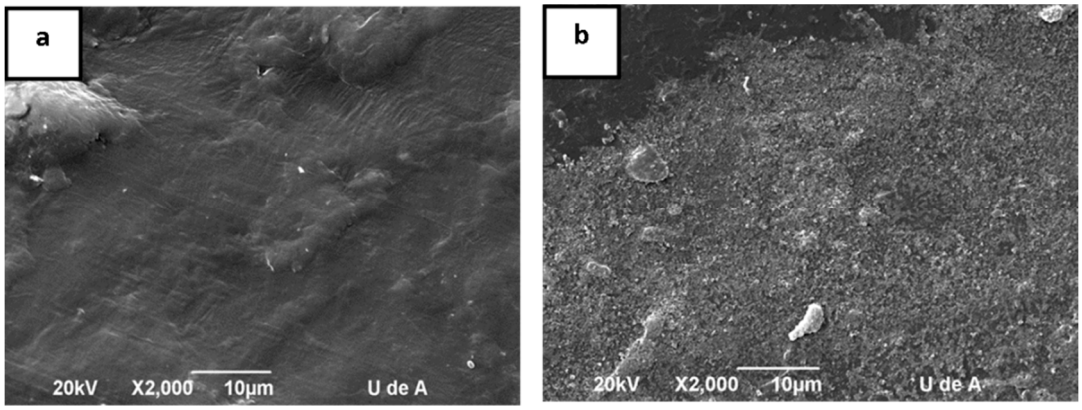

Figure 5. SEM Images of (**a**) bare LDPE pellet and (**b**) TiO_2-LDPE pellet.

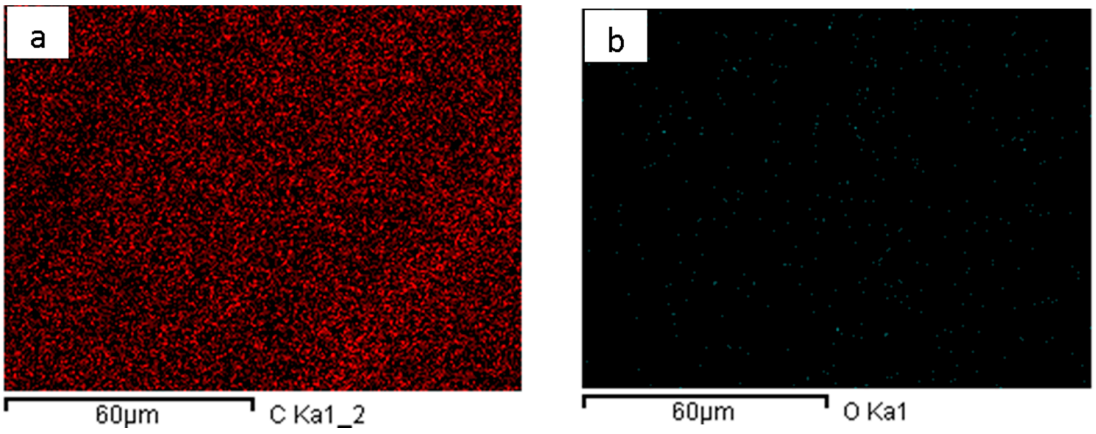

Figure 6. *Cont.*

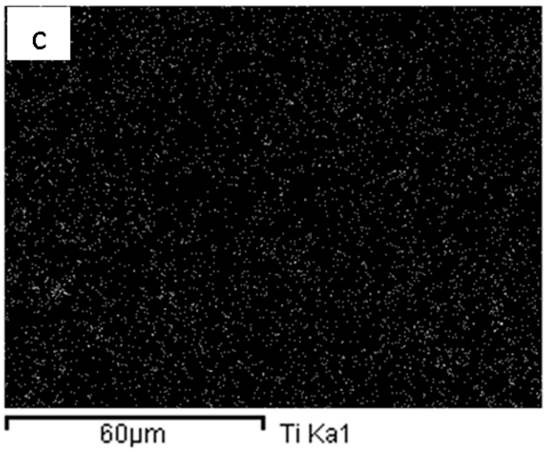

Figure 6. EDS images of TiO_2-LDPE pellet. Distributions of (**a**) C, (**b**) O, and (**c**) Ti.

Erosion test analysis was applied to both kind of substrates, TiO_2-LDPE pellets and TiO_2/SiO_2-BGT, in order to determine the stability of the coatings. The results exhibited that both of the substrates have a good mechanical resistant after 30 min of sonication, showing a good stability of the coating over the substrates. These results are similar to those reported by Velásquez et al. [20] and Matsuzawa [35] for LDPE pellets and BGT, respectively.

3.3. Effects of Solar Radiation and Mechanical Stress on E. coli and Total Bacteria

The photoinactivation and the agitation of the unsupported LDPE pellets under solar radiation in the CPC reactor quickly reduced the *E. coli* concentration during the first 60 min of radiation (Figure 7). After this, inactivation slowed down and it was complete in 120 min with a total UVA dose of energy per unit of volume of 7.22 KJ/L. As expected, total bacteria required more time and radiation dose for complete inactivation (240 min and 20.45 KJ/L) under solar photoinactivation in the flow water through the unsupported LDPE pellets, which is in agreement with other authors [2,10,16]. The inactivation profile of total bacteria during the process was slower than for *E. coli*. Furthermore, Sichel et al. [30] and Van Grieken et al. [16] found similar results due to mechanical stress in reactors in conditions of low osmotic pressure, i.e., within distilled water or in the absence of sufficient saline concentration [17]. The experiments that were carried out in the dark without agitation did not produce any inactivation of the bacteria, this permitted to discriminate any other effect than either photo-inactivation or photocatalytic processes.

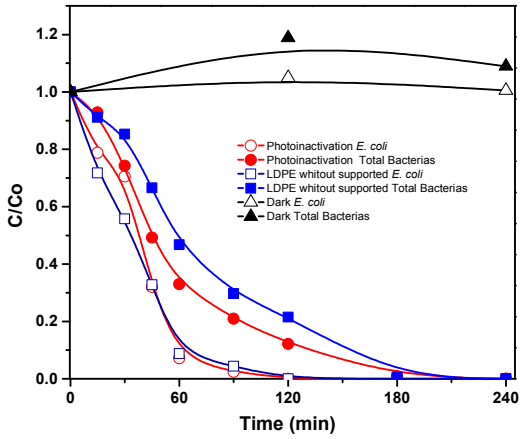

Figure 7. Inactivation of total bacteria and *E. coli* in dark and under sunlight (photoinactivation and mechanical stress caused by agitation of LDPE pellets).

3.4. Photocatalytic Inactivation of Bacteria by Supported TiO_2 Films

Figure 8a,b shows the photocatalytic inactivation of total bacteria and *E. coli* under solar radiation using 50 mg/L of suspended TiO_2, 59 mg/L of TiO_2/SiO_2-BGT and 52 mg·L^{-1} of TiO_2-LDPE pellets. Figure 8a shows similar photocatalytic inactivation results for total bacteria with suspended TiO_2 and TiO_2-LDPE pellets, achieving a viable bacterial concentration reduction of 4.9 log in 180 min of treatment and 11.2 kJ/L of radiation. TiO_2-LDPE pellets led to very similar disinfection results than the suspended catalyst, which was the most efficient due to the optimum contact between bacteria suspension and catalyst. This is in agreement with previous results that were published by Sordo et al. [36]; they found that the use of the fixed-bed wall reactor using TiO_2 immobilized glass rings led to inactivation rates that were quite close to that of the slurry reactor. The main advantage of using the TiO_2-immobilised pellets is the high efficiency for disinfection with easy catalyst recovery. This fact is also very important in the operating costs of the solar photocatalytic treatment [17,37]. The TiO_2/SiO_2-BGT showed lower efficiency, with a viable bacterial concentration reduction of 2 log with the 11.2 kJ/L. This behavior may be related to a smaller available photo-active catalyst surface [14,17].

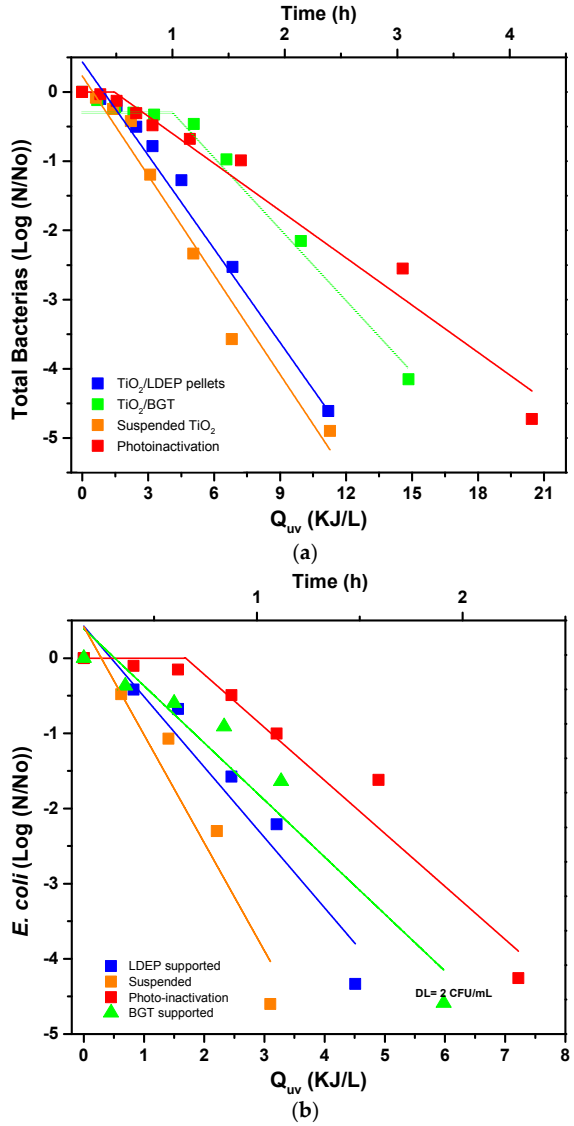

Figure 8. Inactivation of 10^5 CFU/mL of (**a**) total bacteria and (**b**) *E. coli* with suspended TiO_2, TiO_2/SiO_2-BGT, and TiO_2-LDPE pellets.

The bacterial inactivation rates (k) based on the plot of Log(N/No) against solar Q_{UV} for all of the experiments was determined. Three different kinetics models have been used to fit the experimental data obtained: (I) Log-linear model, where the general expression of the Chick-Watson equation was modified for the experimental conditions of this work, time is replaced by the amount of solar UV-A energy received during the experiment per unit volume (Q_{UV}) Equation (2). (II) Shoulder + Log-linear model, when the kinetics present a shoulder in its initial stage, followed by a linear behaviour up to complete disinfection, as proposed by other authors for photocatalytic disinfection [32]. (III) Shoulder + Log lineal + tail; this modification we have used to interpret the kinetics that showed an initial shoulder, a linear section, and a residual tail Equation (4) [38].

$$\mathrm{Log}\frac{N}{No} = -\,k' * Q_{uv} \tag{2}$$

$$\mathrm{Log}\frac{N}{No} = \left\{ \begin{array}{c} 0 \quad ; Q_{uv} \le Q_1 \\ a - \,k'' * Q_{uv;}\,; Q_{uv} > Q_1 \end{array} \right\} \tag{3}$$

$$\mathrm{Log}\frac{N}{No} = \left\{ \begin{array}{c} 0 \quad ; Q_{uv} \le Q_1 \\ a - \,k''' * Q_{uv}; Q_{uv} > Q_1 \\ b \quad ; Q_{uv} \ge Q_1 \end{array} \right\} \tag{4}$$

where N/N_0 is the reduction in the concentration of microorganisms, k' is the kinetic constant inactivation, and Q_{UV} dose is UV-A radiation received at the system per unit of time and volume. Q_1 is the shoulder length, *a* is the logarithm of normalized concentration of microorganism at the point of inflection of the curve and k″ the kinetic constant in the linear section, *b* is the logarithm of the initial concentration of microorganisms (N_0) divided by the residual concentration of microorganisms (N_{res}) (region of the tail of the graph), and k''' is the reaction velocity in the linear zone [38].

The photocatalytic experiments with the 10^5 CFU/mL total bacteria showed that TiO_2-LDPE pellets had a high photocatalytic efficiency, very close to that obtained for suspended TiO_2, evidencing high contact surfaces between TiO_2 and bacteria, Table 3. Results showed the same general tendency, as reported by Gelover et al., 2006, in your disinfection experiments with 100 g immobilized TiO_2 in small Pyrex-glass cylinders [10]. For *E. coli* (Figure 8b and Table 3), as expected, TiO_2 in suspension showed the highest inactivation rate regarding the coated systems, traditionally attributed to a greater catalyst-bacteria contact area, and also to a higher exposed surface area of catalyst available to generate hydroxyl radicals [17,35,37]. *E. coli* achieved the complete inactivation (reaching the detection limit) within 90 min of treatment with the coated systems, 4.5 kJ/L of radiation for TiO_2-LDPE pellets and 5.9 kJ/L for TiO_2/SiO_2-BGT. These treatments were more effective than solar photo-inactivation [1,2,10]. The inactivation observed by mere solar photo-inactivation showed the lowest kinetic, requiring at least 4 h and 2.5 h to achieve the DL for total bacteria and *E. coli*, respectively. These results clearly show that the presence of a photocatalyst, either supported or suspended, accelerates inactivation kinetics rate constants at least twice (Table 3), and reduce the time required to treat the water (reached DL) to 1 h ad 2 h, for *E. coli* and total bacteria, respectively. These results cannot be directly be compared with SODIS results, as this SODIS method is a protocol that requires not only solar exposure of bacteria to solar radiation only, but also to maintain the small water volume (1.5−2 L) static stored for various hours in a PET plastic bottle, as opposite to the reactor functioning on this work.

Table 3. Kinetic data of Total bacteria and *E. coli* photocatalytic experiments with suspended TiO_2, TiO_2/SiO_2-BGT, and TiO_2-LDPE pellets.

Treatment	TiO_2 ($mg \cdot L^{-1}$)	Conc. ($CFU \cdot mL^{-1}$)	k ($L \cdot kJ^{-1}$)	Shoulder Length ($kJ \cdot L^{-1}$)	Log (N_{res})	R^2	Kinetic Model
Total Bacteria							
Photo-inactivation	0	10^5	0.22 ± 0.03	1.56 ± 0.01	–	0.966	Shoulder + Log Linear
TiO_2-suspended	50	10^5	0.47 ± 0.03	–	–	0.967	Log Linear
TiO_2/SiO_2-BGT	59	10^5	0.37 ± 0.01	3.27 ± 0.02	1.17 ± 0.02	0.997	Shoulder + Log Lineal + Tail
TiO_2-LDPE pellets	52	10^5	0.49 ± 0.02	–	–	0.970	Log Linear
E. coli							
Photo-inactivation	0	10^5	0.40 ± 0.10	1.56 ± 0.01	–	0.946	Shoulder + Log Linear
TiO_2-suspended	50	10^5	1.50 ± 0.10	–	–	0.923	Log Linear
TiO_2/SiO_2-BGT	59	10^5	0.46 ± 0.05	–	–	0.954	Log Linear
TiO_2-LDPE pellets	52	10^5	0.90 ± 0.04	–	–	0.910	Log Linear

The most adequate kinetic model for treatment with TiO_2/SiO_2-BGT for total bacteria was adjusted to the 'log-linear' preceded by a shoulder (stationary phase) and followed by a tail (residual concentration), with Log(N_{res}) value of of 1.17, corresponding to the residual bacteria that were left at the end of the treatment in which the limit of detection has not been reached.

The solar photo-inactivation process led to the disinfection of both, *E. coli* and total bacteria, following a shoulder and log-linear kinetic, which could be interpreted as the lag phase of the process until the system receives the energy that is necessary for the microorganisms to start showing the lack of viability as a result of the inactivation due to the self-protection mechanics of the bacteria. This kinetics has lower values for the kinetic parameters as compared with other immobilised TiO_2 systems. Similar results were found Helali et al. for *E. coli* while using suspended TiO_2 [39].

The TiO_2 load of 59 $mg \cdot L^{-1}$ on TiO_2/SiO_2-BGT did not significantly enhance the disinfection rates as compared with the 52 $mg \cdot L^{-1}$ with TiO_2-LDPE pellets, which showed a good fit to the Log-linear model kinetics, due to the high contact area between TiO_2 and bacteria. However, the recovery of TiO_2-LDPE pellets was easy after the treatment, without any after treatment manipulation, which is an important advantage from the practical point of view for the application of this system for water disinfection.

3.5. TiO_2-LDPE Pellets Efficiency at Different Initial Bacterial Concentrations

Figure 9a shows the efficiency of TiO_2-LDPE pellets, under solar radiation, in the inactivation of total bacteria and *E. coli* with different initial concentrations, 10^5, 10^3, 10^1 CFU/mL. The inactivation of total bacteria with an initial concentration of 10^5 CFU/mL was achieved with 11.6 kJ/L of UV-A radiation, while for 10^3 CFU/mL, 8.9 kJ/L of UV-A radiation was needed; meanwhile, 10^1 CFU/mL required 4.2 kJ/L of UV-A radiation. The *E. coli* was more sensitive to the photocatalytic treatment, requiring 4.9 kJ/L of radiation for a concentration of 10^5 CFU/mL, 2.9 kJ/L of radiation for 10^3 CFU/mL and 2.3 kJ/L of radiation for 10^1 CFU/mL (Figure 9b). In both bacteria, disinfection trends were similar and these results are analogous to those that were reported by other authors [40]. According to Craik et al., a fraction of the bacteria may hide from the radiation because of the shielding effect that is generated by higher bacterial concentrations, therefore requiring longer exposure treatments [41]. The results of this work confirm this theory. Table 4 shows the disinfection rates had a similar behavior with the linear log adjustment model, which decreased k values for lower initial bacterial concentrations. The highest kinetic constant was reached for suspended TiO_2 in both total bacteria and *E. coli*.

Finally, bacterial regrowth tests were conducted for photo-inactivation and photocatalysis tests within 24 h after the treatment. Positive regrowth of total coliforms and *E. coli* was found in water treated by photo-inactivation, i.e., without catalyst; while the water that was treated by photocatalysis

did not show any bacterial recovery at all in any of the photocatalytic experiments. Similar recovery results were reported before by other authors, giving the real value of photocatalysis as process for disinfection of water [2,10,14,17,40].

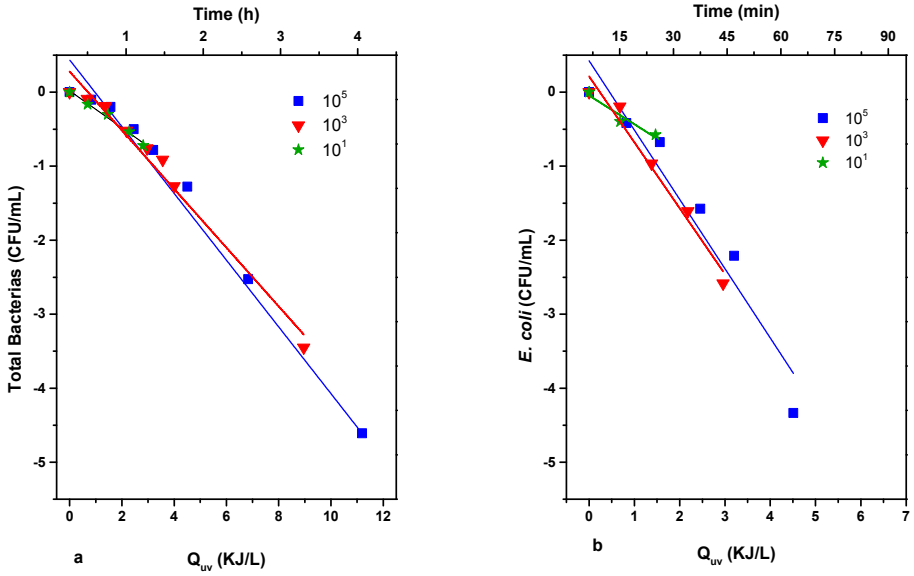

Figure 9. TiO_2-LDPE pellets (52 mg/L) efficiency in the inactivation of different initial concentration of (**a**) total bacteria, (**b**) *E. coli*.

Table 4. Kinetic data of Total bacteria and *E. coli* photocatalytic experiments with TiO_2-LDPE pellets.

Treatment	TiO_2 (mg·L^{-1})	Concentration (CFU·mL^{-1})	k (L·kJ^{-1})	R^2	Kinetic Model
		Total Bacteria			
TiO_2-LDPE pellets	52	10^5	0.49 ± 0.02	0.970	Log Linear
TiO_2-LDPE pellets	52	10^3	0.39 ± 0.03	0.974	Log Linear
TiO_2-LDPE pellets	52	10^1	0.22 ± 0.01	0.977	Log Linear
		E. coli			
TiO_2-LDPE pellets	52	10^5	0.90 ± 0.04	0.891	Log Linear
TiO_2-LDPE pellets	52	10^3	0.89 ± 0.08	0.962	Log Linear
TiO_2-LDPE pellets	52	10^1	0.38 ± 0.10	0.936	Log linear

4. Conclusions

The most effective system for photocatalytic disinfection with solar radiation was TiO_2-LDPE pellets, with photocatalytic disinfection rates that are similar to slurry systems. This system is highly functional because it is easily adapted to the reactor configuration; it is distributed as a dispersed photocatalyst particles and it avoids the catalyst recovery stages, reducing the operational costs.

The optimum time for polymerization and preparing of TiO_2/SiO_2 films on borosilicate glass tubes was 36 h of aging time. Additionally, the thermal analysis revealed that the fist layer of TiO_2-LDPE pellets was the optimal layer for this kind of substrate.

The efficiency of photocatalytic treatment for total bacteria inactivation followed the order, suspended TiO_2/sunlight (50 mg/L) > TiO_2-LDPE pellets/sunlight (52 mg/L) > TiO_2/SiO_2-BGT/sunlight (59 mg/L) > solar photo-inactivation. For the *E. coli* inactivation, similar order was obtained, but TiO_2-LDPE pellets and TiO_2/SiO_2-BGT treatments showed a similar efficiency. Regrowth of total bacteria and *E. coli* microorganisms were not observed 24 h after using any of the photocatalytic treatments that were proposed in this work.

Author Contributions: Data Curation: C.S.; Investigation, Y.A.; Project administration, M.H.; Resources, L.B., Validation, P.F.-I.

Funding: This research was funded by the University of Medellín grant number (2012/00035/002) and the Global Challenges Research Fund and the Research Fund of the United Kingdom for financial support under the SAFEWATER project, GCRF-RCUK grant ref. REF-EP/P032427/1.

Acknowledgments: The authors would like to thank the Universidad de Medellín for financing and supporting this research (2012/00035/002), and the Global Challenges Research Fund and Research Fund UK for the financial support under the SAFEWATER project, GCRF–RCUK grant ref. REF-EP/P032427/1.

Conflicts of Interest: The authors declare no conflicts of interest.

References

1. Lanao, M.; Ormad, M.P.; Mosteo, R.; Ovelleiro, J.L. Inactivation of *Enterococcus* sp. by photolysis and TiO_2 photocatalysis with H_2O_2 in natural water. *Sol. Energy* **2012**, *86*, 619–625. [CrossRef]
2. Rincón, A.-G.; Pulgarin, C. Fe^{3+} and TiO_2 solar-light-assisted inactivation of *E. coli* at field scale. *Catal. Today* **2007**, *122*, 128–136. [CrossRef]
3. Andreozzi, R.; Caprio, V.; Insola, A.; Marotta, R. Advanced oxidation processes (AOP) for water purification and recovery. *Catal. Today* **1999**, *53*, 51–59. [CrossRef]
4. Booshehri, A.Y.; Polo-Lopez, M.I.; Castro-Alférez, M.; Hea, P.; Xu, R.; Rong, W.; Malato, S.; Férnandez-Ibañez, P. Assessment of solar photocatalysis using $Ag/BiVO_4$ at pilot solar Compound Parabolic Collector for inactivation of pathogens in well water and secondary effluents. *Catal. Today* **2017**, *281*, 124–134. [CrossRef]
5. Cruz-Ortiz, B.R.; Hamilton, J.W.J.; Pablos, C.; Díaz-Jiménez, L.; Cortés-Hernández, P.F.-I.D.; Sharma, P.K.; Castro-Alférez, M.; Férnandez-Ibañez, P.; Dunlop, P.S.M.; Byrne, J.A. Mechanism of photocatalytic disinfection using titania-graphene composites under UV and visible irradiation. *Chem. Eng. J.* **2017**, *316*, 179–186. [CrossRef]
6. Castro-Alférez, M.; Polo-López, M.I.; Fernández-Ibáñez, P. Intracellular mechanisms of solar water disinfection. *Sci. Rep.* **2016**, *6*, 38145. [CrossRef]
7. Malato, S.; Fernández-Ibáñez, P.; Maldonado, M.I.; Blanco, J.; Gernjak, W. Decontamination and disinfection of water by solar photocatalysis: Recent overview and trends. *Catal. Today* **2009**, *147*, 1–59. [CrossRef]
8. Mills, A.; Le Hunte, S. An overview of semiconductor photocatalysis. *J. Photochem. Photobiol. A Chem.* **1997**, *108*, 1–35. [CrossRef]
9. Huang, Z.; Maness, P.-C.; Blake, D.M.; Wolfrum, E.J.; Smolinski, S.L.; Jacoby, W.A. Bactericidal mode of titanium dioxide photocatalysis. *J. Photochem. Photobiol. A Chem.* **2000**, *130*, 163–170. [CrossRef]
10. Gelover, S.; Gómez, L.A.; Reyes, K.; Teresa Leal, M. A practical demonstration of water disinfection using TiO_2 films and sunlight. *Water Res.* **2006**, *40*, 3274–3280. [CrossRef] [PubMed]
11. Gelover, S.; Mondragón, P.; Jiménez, A. Titanium dioxide sol–gel deposited over glass and its application as a photocatalyst for water decontamination. *J. Photochem. Photobiol. A Chem.* **2004**, *16*, 241–246. [CrossRef]
12. Pozzo, R.L.; Baltanás, M.A.; Cassano, A.E. Supported titanium oxide as photocatalyst in water decontamination: State of the art. *Catal. Today* **1997**, *39*, 219–231. [CrossRef]
13. Portela, R.; Sánchez, B.; Coronado, J.M.; Candal, R.; Suárez, S. Selection of TiO_2-support: UV-transparent alternatives and long-term use limitations for H_2S removal. *Catal. Today* **2007**, *129*, 223–230. [CrossRef]
14. Turki, A.; Kochkar, H.; García-Fernández, I.; Polo-López, M.I.; Ghorbel, A.; Guillard, C.; Berhault, G.; Fernández-Ibáñez, P. Solar photocatalytic inactivation of Fusarium Solani over TiO_2 nanomaterials with controlled morphology—Formic acid effect. *Catal. Today* **2013**, *209*, 147–152. [CrossRef]
15. Mejía, M.I.; Marín, J.M.; Restrepo, G.; Rios, L.A.; Pulgarín, C.; Kiwi, J. Preparation, testing and performance of a TiO_2/polyester photocatalyst for the degradation of gaseous methanol. *Appl. Catal. B Environ.* **2010**, *94*, 166–172. [CrossRef]
16. Grieken, R.V.; Marugán, J.; Sordo, C.; Pablos, C. Comparison of the photocatalytic disinfection of *E. coli* suspensions in slurry, wall and fixed-bed reactors. *Catal. Today* **2009**, *144*, 48–54. [CrossRef]
17. Alrousan, D.M.A.; Polo-López, M.I.; Dunlop, P.S.M.; Fernández-Ibáñez, P.; Byrne, J.A. Solar photocatalytic disinfection of water with immobilised titanium dioxide in re-circulating flow CPC reactors. *Appl. Catal. B Environ.* **2012**, *128*, 126–134. [CrossRef]

18. Mallak, M.; Bockmeyer, M.; Löbmann, P. Liquid phase deposition of TiO_2 on glass: Systematic comparison to films prepared by sol–gel processing. *Thin Solid Films* **2007**, *515*, 8072–8077. [CrossRef]
19. Song, M.Y.; Park, Y.K.; Jurng, J. Direct coating of V2O5/TiO2 nanoparticles onto glass beads by chemical vapor deposition. *Power Technol.* **2012**, *231*, 135–140. [CrossRef]
20. Velásquez, J.; Valencia, S.; Rios, L.; Restrepo, G.; Marín, J. Characterization and photocatalytic evaluation of polypropylene and polyethylene pellets coated with P25 TiO_2 using the controlled-temperature embedding method. *Chem. Eng. J.* **2012**, *203*, 398–405. [CrossRef]
21. Giovannetti, R.; D'Amato, C.A.; Zannotti, M.; Rommozzi, E.; Gunnella, R.; Miniucci, M.; Di Cicco, A. Visible light photoactivity of polypropylene coated Nano-TiO_2 for dyes degradation in water. *Sci. Rep.* **2015**, *5*, 17801. [CrossRef] [PubMed]
22. Rubio, D.; Casanueva, J.F.; Nebot, E. Improving UV seawater disinfection with immobilized TiO_2: Study of the viability of photocatalysis (UV254/ TiO_2) as seawater disinfection technology. *J. Photochem. Photobiol. A Chem.* **2013**, *271*, 16–23. [CrossRef]
23. Yu, H.; Song, L.; Hao, Y.; Lu, N.; Quan, X.; Chen, S.; Zhang, Y.; Feng, Y. Fabrication of pilot-scale photocatalytic disinfection device by installing TiO_2 coated helical support into UV annular reactor for strengthening sterilization. *Chem. Eng. J.* **2016**, *283*, 1506–1513. [CrossRef]
24. Ratova, M.; Mills, A. Antibacterial titania-based photocatalytic extruded plastic films. *J. Photochem. Photobiol. A Chem.* **2015**, *299*, 159–165. [CrossRef]
25. Rtimi, S.; Sanjines, R.; Andrzejczuk, M.; Pulgarin, C.; Kulik, A.; Kiwi, J. Innovative transparent non-scattering TiO_2 bactericide thin films inducing increased *E. coli* cell wall fluidity. *Surf. Coat. Technol.* **2014**, *254*, 333–343. [CrossRef]
26. Yemmireddy, V.K.; Hung, Y.C. Photocatalytic TiO_2 coating of plastic cutting board to prevent microbial cross-contamination. *Food Control* **2017**, *77*, 88–95. [CrossRef]
27. Yañez, D.; Guerrero, S.; Lieberwirth, I.; Ulloa, M.T.; Gomez, T.; Rabagliati, F.M.; Zapata, P.A. Photocatalytic inhibition of bacteria by TiO_2 nanotubes-doped polyethylene composites. *Appl. Catal. A Gen.* **2015**, *489*, 255–261. [CrossRef]
28. Bahloul, W.; Mélis, F.; Bounor-Legaré, V.; Cassagnau, P. Structural characterisation and antibacterial activity of PP/TiO_2 nanocomposites prepared by an in situ sol–gel method. *Mater. Chem. Phys.* **2012**, *134*, 399–406. [CrossRef]
29. Marín, J.M.; Fidelgranda, C.; Galeano, L.; Rios, L.A.; Restrepo, G. Impregnación de TiO_2 sobre borosilicato por el método sol-gel usando inmersión a velocidad controlada. *Sci. Tech.* **2007**, *2*, 441–446.
30. García-Fernández, I.; Polo-López, M.I.; Oller, I.; Fernández-Ibáñez, P. Bacteria and fungi inactivation using Fe^{3+}/sunlight, H_2O_2/sunlight and near neutral photo-Fenton: A comparative study. *Appl. Catal. B Environ.* **2012**, *121–122*, 20–29. [CrossRef]
31. Lei, P.; Wang, F.; Gao, X.; Ding, Y.; Zhang, S.; Zhao, J.; Liu, S.; Yang, M. Immobilization of TiO_2 nanoparticles in polymeric substrates by chemical bonding for multi-cycle photodegradation of organic pollutants. *J. Hazard. Mater.* **2012**, *227–228*, 185–194. [CrossRef] [PubMed]
32. Safajou, H.; Khojasteh, H.; Salavati-Niasari, M.; Mortazavi-Derazkola, S. Enhanced photocatalytic degradation of dyes over graphene/Pd/ TiO_2 nanocomposites: TiO2 nanowires versus TiO2 nanoparticles. *J. Colloid Interface Sci.* **2017**, *498*, 423–432. [CrossRef] [PubMed]
33. León, A.; Reuquen, P.; Garín, C.; Segura, R.; Vargas, P.; Zapata, P.; Orihuela, P.A. FTIR and raman characterization of TiO_2 nanoparticles coated with Polyethylene Glycol as carrier for 2-Methoxyestradiol. *Appl. Sci.* **2017**, *7*, 49. [CrossRef]
34. Fischer, E.W. Effect of annealing and temperature on the morphological structure of polymers. *Pure Appl. Chem.* **1972**, *31*, 113–132. [CrossRef]
35. Matsuzawa, S.; Maneerat, C.; Hayata, Y.; Hirakawa, T.; Negishi, N.; Sano, T. Immobilization of TiO_2 nanoparticles on polymeric substrates by using electrostatic interaction in the aqueous phase. *Appl. Catal. B Environ.* **2008**, *83*, 39–45. [CrossRef]
36. Sordo, C.; Van Grieken, R.; Marugán, J.; Fernández-Ibáñez, P. Solar photocatalytic disinfection with immobilised TiO2 at pilot-plant scale. *Water Sci. Technol.* **2010**, *61*, 507. [CrossRef] [PubMed]
37. Hincapié, M.; Balaguera, A.; Botero, L.; Sánchez, C.; Restrepo, G.; Marín, J. Purificación del agua por fotocatálisis. In *Even. X Jornadas Investig. Univ. Medellín INNOVACIÓN Y Transf. Conoc. EN Ing.*; Sello Editorial Universidad de MedellSín: Medellín, Colombia, 2014; pp. 75–92.

38. Marugán, J.; Grieken, R.V.; Sordo, C.; Cruz, C. Kinetics of the photocatalytic disinfection of Escherichia coli suspensions. *Appl. Catal. B Environ.* **2008**, *82*, 27–36. [CrossRef]
39. Helali, S.; Polo-López, M.I.; Fernández-Ibáñez, P.; Ohtani, B.; Amano, F.; Malato, S.; Guillard, C. Solar photocatalysis: A green technology for E. coli contaminated water disinfection. Effect of concentration and different types of suspended catalyst. *J. Photochem. Photobiol. A Chem.* **2014**, *276*, 31–40. [CrossRef]
40. Rincón, A.G.; Pulgarin, C. Bactericidal action of illuminated TiO_2 on pure Escherichia coli and natural bacterial consortia: post-irradiation events in the dark and assessment of the effective disinfection time. *Appl. Catal. B Environ.* **2004**, *49*, 99–112. [CrossRef]
41. Craik, S.A.; Weldon, D.; Finch, G.R.; Bolton, J.R.; Belosevic, M. Inactivation of cryptosporidium parvum oocysts using medium- and low-pressure ultraviolet radiation. *Water Res.* **2001**, *35*, 1387–1398. [CrossRef]

© 2018 by the authors. Licensee MDPI, Basel, Switzerland. This article is an open access article distributed under the terms and conditions of the Creative Commons Attribution (CC BY) license (http://creativecommons.org/licenses/by/4.0/).